Structural Engineering and Mechanics, Vol. 34, No. 5 (2010) 563-580
DOI: http://dx.doi.org/10.12989/sem.2010.34.5.563

Behavior of strengthened reinforced concrete coupling beams by bolted steel plates, Part 2: Evaluation of theoretical strength

Y. Zhu[1] and R.K.L. Su[2*]

[1]*School of Civil Engineering, The University of Guang Zhou, China*
[2]*Department of Civil Engineering, The University of Hong Kong, Hong Kong, China*

(Received August 23, 2007, Accepted November 16, 2009)

Abstract. Composite beams using bolts to attach steel plates to the side faces of existing reinforced concrete (RC) coupling beams can enhance both their strength and deformability. The behavior of those composite beams differs substantially from the behavior of typical composite beams made up of steel beams and concrete slabs. The former are subjected to longitudinal, vertical and rotational slips, while the latter only involve longitudinal slip. In this study, a mixed analysis method was adopted to develop the fundamental equations for accurate prediction of the load-carrying capacity of steel plate strengthened RC coupling beams. Then, a rigid plastic analysis technique was used to cope with the full composite effect of the bolt group connections. Two theoretical models for the determination of the strength of medium-length plate strengthened coupling beams based on mixed analysis and rigid plastic methods are presented. The strength of the strengthened coupling beams is derived. The vertical and longitudinal slips of the steel plates and the shear strength of the anchor-bolt connection group is considered. The theoretical models are validated by the available experimental results presented in a companion paper. The strength of the specimens predicted from the mixed analysis model is found to be in good agreement with that from the experimental results.

Keywords: coupling beam; strengthening; steel plate; bolt connection; slip strain; partial interaction; rigid plastic; mixed analysis.

1. Introduction

In the past two decades, strengthening and stiffening of reinforced concrete (RC) beams and slabs using bolting and adhesive bonding steel plates on their tension faces have been widely adopted in the practice of retrofitting and repairing buildings and other infrastructures (Oehlers 1992). However, adding steel plates to the tension faces of beams or slabs can lead to over-reinforcement and potentially brittle failure. On the other hand, bolting steel plates to the side faces of RC beams can enhance both strength and deformability but without any loss of ductility, particularly when the plates are extended into the compression regions of the beams (Zhu *et al.* 2007).

Fig. 1(a) shows a typical configuration of a plate-strengthened RC coupling beam. The

*Corresponding author, Associate Professor, E-mail: klsu@hkucc.hku.hk

deformation of the beams with full and partial interactions of the bolt connectors are depicted in Fig. 1(b) and Fig. 1(c) respectively. Shear connectors are normally symmetrically distributed about the centroid of the plate element at the ends of coupling beams. The behavior of composite beams displayed in Fig. 1 differs substantially from that of typical composite floor beams which consist of

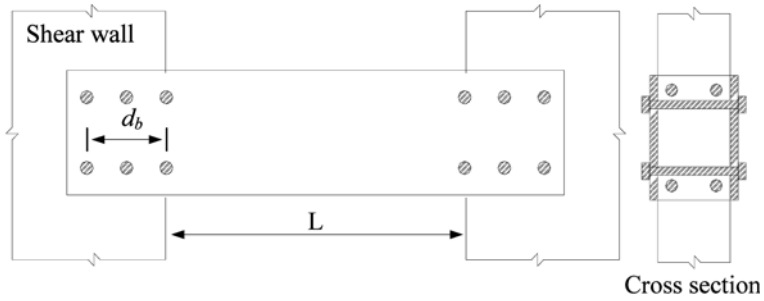

(a) Plated RC coupling beam

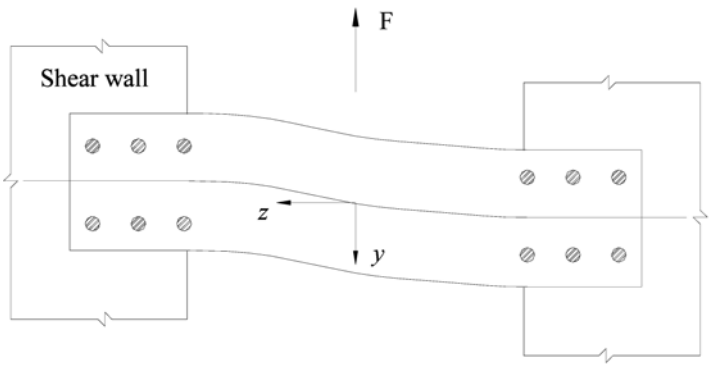

(b) Full interaction

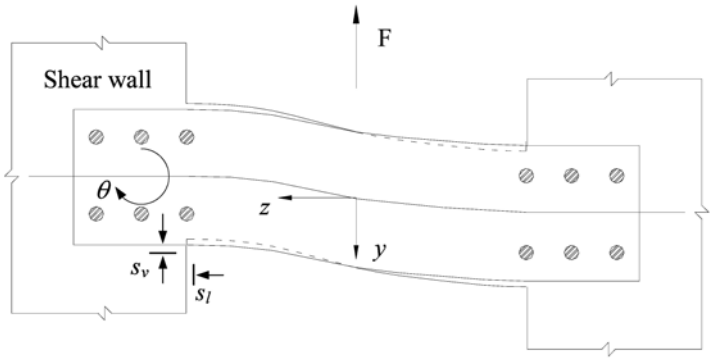

(c) Longitudinal and vertical partial interaction

Fig. 1 Full and partial interaction

steel beams and concrete slabs (Oehlers and Bradford 1995, 1999). This is because the latter is only subjected to longitudinal slip whereas the former is subjected to both longitudinal and vertical slips as well as rotational slip (Zhu *et al.* 2007). Oehlers and Sved (1995) studied the fracture of shear connectors in side-plate strengthened floor beams and proposed a mixed analysis method for modeling which assumed that both concrete and steel elements remain linearly elastic whereas all the shear connectors undergo plastic deformation when they are fully loaded. In this theoretical study, the bolt shear connectors are assumed to transfer the shear by dowel action. Hence, any beneficial effect of friction will be ignored. The partial interaction model (Newmark *et al.* 1951, Johnson 1994, Oehlers *et al.* 1997) will be extended to build the fundamental equations for side plated coupling beams which have different boundary, loading and bolt connection arrangement conditions. Then a rigid plastic analysis technique (Oehlers and Bradford 1995) will be adopted to cope with the longitudinal and vertical slips in bolted side plated coupling beams. The associated problems of avoiding local buckling failure of the steel plate have been mentioned in the companion paper (Zhu *et al.* 2007) and will not be considered in the following theoretical development.

This study presents two theoretical models for determination of the strength of strengthened coupling beams with a span-to-depth ratio larger than 2 based on the mixed analysis method and the rigid plastic method. The load capacity of the strengthened coupling beams will consider steel plates with vertical and longitudinal slips as well as the shear strength demand of the anchor-bolt connection group. The theoretical results will be compared with the available experimental results to validate the theories.

2. Mixed analysis method

The mixed analysis method proposed by Oehlers and Sved (1995) was extended to model steel plate strengthened coupling beams to calculate the vertical slip and longitudinal slip between concrete and steel plates. Three cases with various idealized connection conditions between the plates and concrete are considered. They are (i) longitudinal-full-interaction and vertical-full-interaction, (ii) longitudinal-partial-interaction and vertical-full-interaction, and (iii) longitudinal-partial-interaction and vertical-partial-interaction. The three cases will be analyzed separately in the following sections.

2.1 Case 1: Longitudinal-full-interaction and vertical-full-interaction

Full-interaction occurs when the strain profile through the concrete element is parallel and coincides with the strain profile through the steel plate element as shown in Fig. 2, whereas partial-interaction is defined as when the strain profiles do not coincide. The term full-shear-connection strength is defined as the strength P_{fsc} of the shear connection in a strengthened coupling beam that is required to achieve the maximum theoretical flexural capacity of the composite beam. For simplicity, the plates on both sides of the beam will be theoretically treated as an equivalent single plate of thickness $2t_p$.

As illustrated in Fig. 2, the moments acting at the equivalent plate element and at the concrete element are defined as M_p and M_{RC} respectively. The applied moment acting at the beam-wall joint is $M_{app} = FL/2$ where L is the span length of the coupling beam.

Based on the assumption of full-interaction between the plate and the concrete elements, their

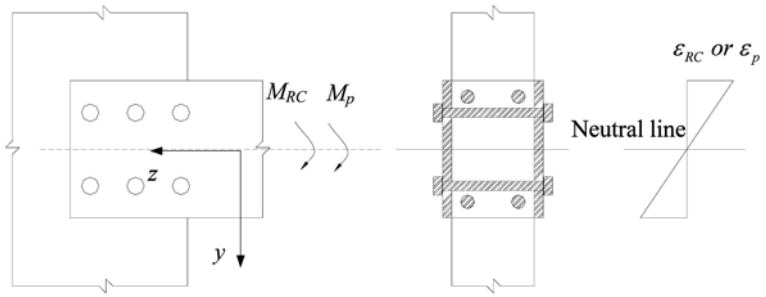

Fig. 2 Full interaction

neutral axes coincide and therefore there is no slip-strain between the strain profiles ε_c of the concrete and ε_p of the steel plate. Thus, the curvatures of the plate element κ_p and concrete element κ_c are the same as shown in Fig. 2. Considering compatibility of the curvatures, Eq. (1) can be obtained

$$\frac{(M_{RC})_z}{(EI_{RC})_z} = \frac{(M_p)_z}{(EI_p)_z} = \frac{(M_{RC})_z + (M_p)_z}{(EI_{RC})_z + (EI_p)_z} \tag{1}$$

where $(EI)_{RC}$ and $(EI)_p$ are flexural rigidities of the RC and plate elements respectively. The symbol $(\bullet)_z$ denotes that the quantity inside the bracket is a function of z. From equilibrium of the moments (shown in Fig. 2), we have

$$(M_{app})_z = (M_{RC})_z + (M_p)_z \tag{2}$$

According to Eqs. (1) and (2) and substituting m for $(EI)_{RC}/(EI)_p$, gives

$$(M_{p,fi})_z = \frac{(M_{app})_z}{m+1} \tag{3}$$

$$(M_{RC,fi})_z = \frac{m(M_{app})_z}{m+1} \tag{4}$$

It can be clearly seen from the above two equations that when the composite action of the strengthened coupling beam is in full-interaction, the internal forces in the concrete element and steel element will be proportional to the ratio of their stiffness. However, the plates are connected to concrete by bolts and they resist the interface shear by mechanical action which must slip in order to mobilize the action. The slip reaches its maximum at the position of maximum moment. Therefore, even when the strength of the shear connection is sufficient to take up all the force arising from the full-shear-connection, there must be partial-interaction like that shown in Fig. 3 and Fig. 4. Another way of visualizing the problem is that if the plates were adhesively bonded to the beam, then a state of full interaction would exist in which case the plated beam could achieve its maximum theoretical flexural capacity. However, bolted connectors are mechanical shear connectors that require slip to develop the resisting shear. Hence coupling beams strengthened with bolted plates are not possible to achieve their maximum theoretical flexural capacity derived from full composite interactions.

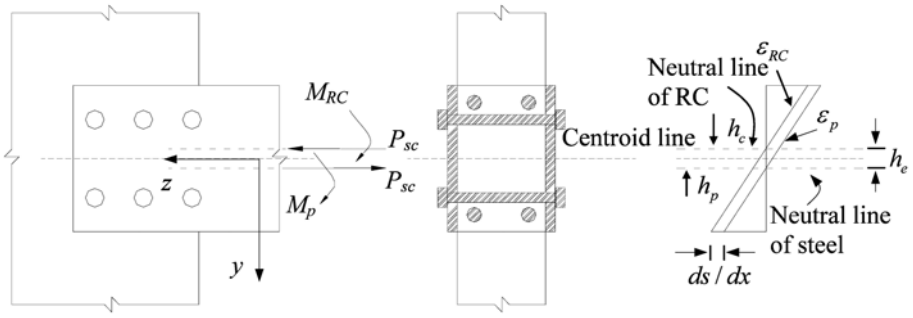

Fig. 3 Longitudinal partial and vertical full interactions

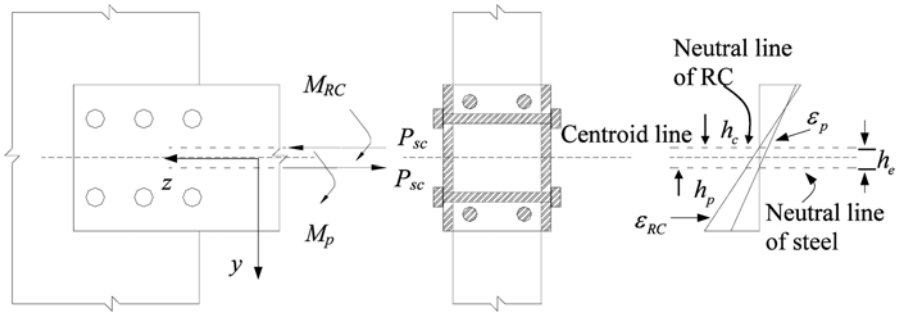

Fig. 4 Longitudinal partial and vertical partial interactions

2.2 Case 2: Longitudinal-partial-interaction and vertical-full-interaction

The vertical shear force taken by the steel plates will be determined in this section. In this case, it is assumed that the composite action of the strengthened beams is longitudinal-partial-interaction and vertical-full-interaction (i.e., allows longitudinal slip but not transverse slip) as shown in Fig. 3. In this case, as the neutral axes of concrete and steel plates do not coincide, there is a slip-strain *ds/dz* (Oehlers and Bradford 1995, Oehlers *et al.* 1997) between the strain profiles ε_c and ε_p of the elements. The curvatures of the plate element κ_p and concrete element κ_c are the same, as there is only a longitudinal slip. Owing to the anti-symmetric arrangement of the applied loads at both ends of the beam, the longitudinal slip between the steel plate and concrete must be zero at mid-span and the maximum longitudinal slip occurs at the beam-wall joint near the shear connections. Integrating the slip-strain along the half span of the coupling beam gives the total (maximum) longitudinal slip s_l.

Because of the slip, an axial tensile force of P_{sc} develops in the plate element and an axial compressive force of the same magnitude is generated in the concrete element. These forces act at the neutral axes of the elements, which are at a distance h_e apart. The total strength of the shear connectors at one end of the equivalent steel plate is defined as P_{sc}. From equilibrium of the moments as shown in Fig. 3

$$(M_{app})_z = (M_{RC})_z + (M_p)_z - P_{sc}(h_e)_z \tag{5}$$

Comparing Eq. (2) to Eq. (5), it can be seen that the longitudinal slip reduces the load-carrying capacity of the strengthened coupling beams.

Substituting Eq. (1) and $m = (EI)_{RC}/(EI)_p$ into Eq. (5), gives

$$(M_{p,vfi})_z = \frac{(M_{app})_z + P_{sc}(h_e)_z}{m+1} \tag{6}$$

$$(M_{RC,vfi})_z = \frac{m[(M_{app})_z + P_{sc}(h_e)_z]}{m+1} \tag{7}$$

where the subscript *vfi* in the equations denotes that vertical-full-interaction is being considered in the analysis.

As shown in Fig. 3, the distances of the neutral axes of the concrete element and plate element to the centroid of the combined section are h_c and h_p respectively. Based on the definition of slip strains and taking into account the internal forces acting on the shear span z from mid-span of the coupling beam as shown in Fig. 1(c), the slip strain at the centroid of the section can be expressed as

$$\frac{ds_l}{dz} = \varepsilon_c - \varepsilon_p = \frac{-M_{RC}h_c}{(EI)_{RC}} - \frac{-M_p h_p}{(EI)_p} \tag{8}$$

Noting from Fig. 3 that $h_p - h_c = h_e$ and that $M_{RC}/(EI)_{RC} = M_p/(EI)_p$, and considering M_p from Eq. (6), the slip strain under the condition of vertical-full-interaction

$$\left(\frac{ds_l}{dz}\right)_{vfi} = M_{app}\frac{h_e}{\Sigma(EI)} + P_{sc}\frac{h_e^2}{\Sigma(EI)} \tag{9}$$

Note that in the preceding equations, the sign of the distances h_c and h_p depends on the location of the neutral axes of the elements. The sign is negative when the neutral axis is located in the negative side of the vertical coordinate and positive when it is located in the positive side of the vertical coordinate. Here, the origin of the vertical coordinate is defined at the centroid of the combined section.

At the cross-section of a distance z from mid-span of the beam as shown in Fig. 1(c), the moment of the cross-section is

$$(M_{app})_z = Fz \tag{10}$$

The main objective of this study is to develop an analytical tool for determining the strength of medium-length plate strengthened coupling beams It is assumed that steel and concrete materials are linearly elastic and the notional stiffness is constant along the coupling beam due to the fact that only a few minor cracks and local damage were observed during our previous experimental study of strengthened coupling beams at the ultimate loading state (Zhu *et al.* 2007). The moments $(M_{RC})_z$ and $(M_p)_z$ vary linearly along the span of the beam as shown in Fig. 1. Hence, the separation h_e of the neutral axes is also a linear function of the span. Denoting $h_e^{\max}$ as the maximum h_e at the beam-wall joint ($z = L/2$), h_e can be expressed as

$$h_e = \frac{h_e^{\max} z}{L/2} \tag{11}$$

Substituting Eqs. (10) and (11) into Eq. (9) and simplifying, gives

$$\left(\frac{ds_l}{dz}\right)_{vfi} = F\frac{h_e^{\max}}{0.5L\Sigma(EI)}z^2 + P_{sc}\frac{(h_e^{\max})^2}{0.25L^2\Sigma(EI)}z^2 \tag{12}$$

Integrating Eq. (12) produces the longitudinal slip distribution along the span z as

$$s_l(z) = \left\{F\frac{h_e^{\max}}{0.5L\Sigma(EI)} + P_{sc}\frac{(h_e^{\max})^2}{0.25L^2\Sigma(EI)}\right\}\frac{z^3}{3} \tag{13}$$

This longitudinal slip variation is a cubic function of z with a maximum value at the beam-wall joint and zero at mid-span (where $z = 0$) owing to the anti-symmetry deformation of the coupling beam under the given loading condition.

The maximum longitudinal slip at the beam-wall joint can be obtained by substituting $z = L/2$ in Eq. (13). Hence

$$(s_{l,\max})_{vpi} = F\frac{h_e^{\max}L^2}{12\Sigma(EI)} + P_{sc}\frac{(h_e^{\max})^2 L}{6\Sigma(EI)} \tag{14}$$

Given that V_{fi} is the vertical shear force in the shear connections when there is full-vertical-interaction and d_b is the horizontal dimension of the group of shear connectors as shown in Fig. 1(a), the moment at the joints of the plate can be estimated by Eq. (15)

$$(M_{p,vfi})_{joint} = V_{fi}d_b \tag{15}$$

Substituting Eq. (15) into Eq. (6) and considering the location of the beam-wall joint ($z = L/2$)

$$V_{fi} = \frac{0.5FL + P_{sc}h_e^{\max}}{(m+1)d_b} \tag{16}$$

Eq. (16) gives the upper bound of the vertical force in the shear connectors which will reduce to zero as the degree of vertical-partial-interaction reduces to zero.

2.3 Case 3: Longitudinal-partial-interaction and vertical-partial-interaction

Consider the strengthened coupling beam with both longitudinal and vertical-partial-interactions between the plate and concrete elements as shown in Fig. 4. In this case, the element curvatures κ_c and κ_p in the figure are not the same. If the difference in element curvatures is $\Delta\kappa$, then

$$\Delta\kappa = \kappa_c - \kappa_p = \frac{M_{RC,vpi}}{(EI)_{RC}} - \frac{M_{p,vpi}}{(EI)_p} \tag{17}$$

where the subscript *vpi* refers to vertical-partial-interaction.

Similar to the last section, the difference of the element curvatures $\Delta\kappa$ is also a linear function with respect to the span. As $\Delta\kappa_{\max}$ is a maximum at the beam-wall joint ($z = L/2$) and $\Delta\kappa = 0$ at the mid-span of the coupling beam ($z = 0$), hence

$$\Delta\kappa = \frac{\Delta\kappa_{\max}z}{L/2} \tag{18}$$

From Eqs. (5), (10), (11) (17) and (18), the moments acting at the concrete and steel elements when there is vertical-partial-interaction can be derived as

$$(M_{RC,vpi})_z = \frac{[m(F + 2P_{sc}h_e^{\max}L^{-1}) + 2\Delta\kappa_{\max}L^{-1}(EI)_{RC}]z}{m+1} = F_c'z \tag{19}$$

$$(M_{p,vpi})_z = \frac{[F + 2P_{sc}h_e^{\max}L^{-1} - 2\Delta\kappa_{\max}L^{-1}(EI)_{RC}]z}{m+1} = F_p'z \tag{20}$$

Assuming the shear forces induced by vertical-partial-interaction are conservatively resisted by the outermost columns of the bolts and letting V_{pi} be the vertical shear force acting on the connectors at one column of the anchor-bolt connections when there is vertical-partial-interaction, from Fig. 1(a)

$$(M_{p,vpi})_{L/2} = V_{pi}d_b \tag{21}$$

Applying Eq. (20) at $z = L/2$, substituting into Eq. (21) and rearranging gives

$$V_{pi} = \frac{F + 2P_{sc}h_e^{\max}L^{-1} - 2\Delta\kappa_{\max}L^{-1}(EI)_{RC}}{m+1}\frac{L}{2d_b} = F_p'\frac{L}{2d_b} \tag{22}$$

Further substituting Eq. (16) into Eq. (22) gives

$$V_{pi} = V_{fi} - \frac{\Delta\kappa_{\max}}{d_b((EI)_{RC}^{-1} + (EI)_P^{-1})} = V_{fi} - \frac{\Delta\kappa_{\max}}{d_b\Sigma(EI)^{-1}} \tag{23}$$

In the following paragraphs, the relationship between the vertical displacement distribution of the elements along the shear span are analyzed.

Dividing Eqs. (19) and (20) by the flexural rigidity of their elements give the following variations in curvatures of each element

$$\frac{d^2y_c}{dz^2} = \frac{F_c'z}{(EI)_{RC}} \tag{24}$$

$$\frac{d^2y_p}{dz^2} = \frac{F_p'z}{(EI)_p} \tag{25}$$

where y_c and y_p are the vertical displacements of the concrete and plate elements respectively whereas the constants F_c' and F_p' are defined in Eqs. (19) and (20). The longitudinal or vertical slip of the bolts at mid-span must be zero as the coupling beam is anti-symmetric under the applied load, and the maximum longitudinal or vertical slip occurs at the beam-wall joints near the anchor-bolt connections.

As an anti-symmetric load is applied to the coupling beam as shown in Fig. 1(a), the vertical displacements at mid-span and the slopes at beam-wall joints are zero, meaning that at $z = 0$, $y = 0$ and at $z = L/2$, $dy/dz = 0$. Integrating Eq. (24) twice gives the following variation in vertical displacements

$$y_c(z) = \left(\frac{z^3}{6} - \frac{L^2z}{8}\right)\frac{F_c'}{(EI)_{RC}} \tag{26}$$

However, since the bolt group rotates under the applied moment $M_{p,vpi}$, there is a rotation angle θ at the section of beam-wall joints. So the vertical displacements at mid-span is zero and the slopes at beam-wall joints is $-\theta$, meaning that $z = 0$, $y = 0$ and $z = L/2$, $dy/dz = -\theta$. Then integrating Eq. (25) twice gives the following variation in vertical displacements

$$y_p(z) = \left(\frac{z^3}{6} - \frac{L^2 z}{8}\right)\frac{F_p'}{(EI)_p} - \theta z \tag{27}$$

The displacement difference obtained by subtracting Eq. (27) from (26) is the vertical slip s_v between the elements. Hence

$$s_v(z) = \left(\frac{z^3}{6} - \frac{L^2 z}{8}\right)\left(\frac{F_c'}{(EI)_{RC}} - \frac{F_p'}{(EI)_p}\right) + \theta z \tag{28}$$

which has the maximum value at the beam-wall joint ($z = L/2$)

$$s_v\left(\frac{L}{2}\right) = \frac{L^3}{24}\left(\frac{F_c'}{(EI)_{RC}} - \frac{F_p'}{(EI)_p}\right) + \frac{L\theta}{2} \tag{29}$$

Furthermore, substituting the values of F_c' and F_p' from Eqs. (19) and (20) into Eq. (29) gives

$$s_{v,\max} = -\frac{\Delta\kappa_{\max} L^2}{12} + \frac{L\theta}{2} \tag{30}$$

Noting that θ is defined as $M_{p,vpi}/K_{r,bolt}$ and $K_{r,bolt}$ is the rotational stiffness of the bolt groups at the ends of the beam.

Taking into account the partial interaction actions as shown in Fig. 4 and noting that $h_p - h_c = h_e$ and $M_{RC}/(EI)_{RC} = M_p/(EI)_p + \Delta\kappa$, the equation for the slip strain at the centroid of the section as expressed in Eq. (8) can be further simplified as

$$\frac{ds_l}{dz} = \frac{M_p h_e}{(EI)_p} - \Delta\kappa h_e \tag{31}$$

Substituting M_p from Eq. (20) into Eq. (31) and rearranging yields

$$\frac{ds_l}{dz} = M_{app}\frac{h_e}{\Sigma(EI)} + P_{sc}\frac{h_e^2}{\Sigma(EI)} - \Delta\kappa h_e\left(\frac{(EI)_{RC}}{\Sigma(EI)} + 1\right) \tag{32}$$

Substituting Eq. (9) into Eq. (32) produces

$$\left(\frac{ds_l}{dz}\right)_{vpi} = \left(\frac{ds_l}{dz}\right)_{vfi} - \Delta\kappa h_e\left(\frac{(EI)_{RC}}{\Sigma(EI)} + 1\right) \tag{33}$$

It can be concluded from Eq. (33) that the slip strain under the condition of vertical-partial-interaction is directly proportional to that due to vertical-full-interaction and the difference between the RC and plate curvatures times the difference between the RC and plate element neutral axes. Note that the signs of h_c and h_p have been defined in section 2.2.

According to Eqs. (10), (11) and (12), Eq. (32) can be re-written as

$$\frac{ds_l}{dz} = F\frac{h_e^{\max}}{0.5L\Sigma(EI)}z^2 + P_{sc}\frac{(h_e^{\max})^2}{0.25L^2\Sigma(EI)}z^2 - \frac{\Delta\kappa_{\max}}{0.5L}\frac{h_e^{\max}}{0.5L}z^2\left(\frac{(EI)_{RC}}{\Sigma(EI)} + 1\right) \tag{34}$$

Integrating Eq. (34) produces the longitudinal slip distribution along the span z as

$$s_l(z) = F\frac{h_e^{\max}}{1.5L\Sigma(EI)}z^3 + P_{sc}\frac{(h_e^{\max})^2}{0.75L^2\Sigma(EI)}z^3 - \frac{\Delta\kappa_{\max}}{0.5L}\frac{h_e^{\max}}{1.5L}z^3\left(\frac{(EI)_{RC}}{\Sigma(EI)} + 1\right) \tag{35}$$

It can be seen that the longitudinal slip variation is a cubic polynomial of z with a maximum at the beam-wall joints and zero at mid-span (where $z = 0$) owing to the anti-symmetry deformation of the coupling beam under the applied load.

The maximum longitudinal slip at the beam-wall joint can be obtained by substituting $z = L/2$ in Eq. (35). Hence

$$(s_{l,\max})_{vpi} = \frac{(M_{RC} + M_p)h_e^{\max}L}{6\Sigma(EI)} - \frac{\Delta\kappa_{\max}h_e^{\max}L}{6}\left(\frac{(EI)_{RC}}{\Sigma(EI)} + 1\right) \tag{36}$$

In this section, assuming the composite action of partial-longitudinal and partial vertical interactions, the vertical slip and longitudinal slip can be computed by Eqs. (28) and (35) respectively.

3. Rigid plastic method

Using the rigid plastic method, an upper bound analysis was conducted to determine the load-carrying capacity of plate strengthened RC coupling beams. The analysis assumes that the three components of the composite beam (i.e., the steel, the concrete and the shear connectors) have unlimited ductility and hence each of them can reach and maintain their plastic or yield strengths. When there is full-shear-connection and full-longitudinal and vertical-interactions, the strain profiles of the RC component and the steel plate are assumed to be parallel and coincident as shown in Fig. 5. As the materials are assumed to be rigid plastic, the RC and steel elements have the stress distributions as displayed in Figs. 5(b) and 5(c) respectively. It is necessary to determine the position of the neutral axis, x, where the total compressive force from the concrete, reinforcing bars and the steel plate above the neutral axis is equal to the sum of tensile forces from the steel plate and reinforcing bars below the neutral axis. Having determined the position of the neutral axis and hence the distribution of stresses, the stresses can be integrated over the areas which they act to determine the forces in the RC beam and in the steel plate. The resultant force in the plate element, which will also be the resultant force in the RC element, is equal to the shear capacity of the bolt groups required for a full-shear-connection P_{sc}. The moment capacity can be determined by taking a moment of the forces about any convenient axis, such as the neutral axis.

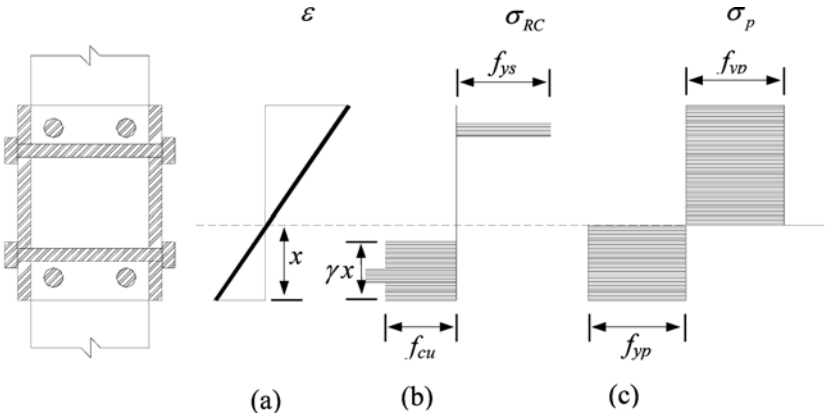

Fig. 5 Full shear connection and interaction analyses

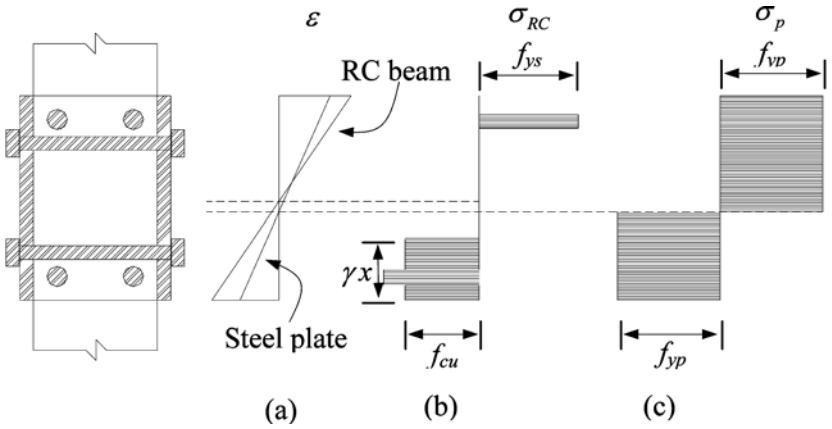

Fig. 6 Partial shear connection and interaction analyses

If the provided strength P_{psc} of the shear connection is less than that required for the full-shear-connection P_{sc}, then the load-carrying capacity of the strengthened coupling beam can be determined from a partial-shear-connection and partial-interaction analyses as depicted in Fig. 6. In the case that the strain profiles in Fig. 6(a) do not coincide, it needs to find the position of the neutral axis in the RC element where the resultant force is P_{psc} such that the strain profiles of RC element and steel plates are the same. Once the neutral axes, and hence the stress distribution, have been determined, the load-carrying capacity of the composite beam can be determined in the usual way.

4. Strength of bolted side steel plate strengthened coupling beam

4.1 Strength analysis of strengthened coupling beam

The theoretical ultimate shear capacity (V_u^*) of the strengthened coupling beam specimens is derived from the combination of the mixed analysis method and the rigid plastic method. The following assumptions are made in the calculations:

(1) Plane sections remain plane after bending.
(2) The longitudinal reinforcement and the concrete are perfectly bonded together.
(3) The steel plates of the strengthened coupling beams are anchored into the wall piers at each end.
(4) The plate thickness is dimensioned so that buckling is avoided.
(5) Tensile strength of cracked concrete is neglected.
(6) The longitudinal reinforcement and steel plates are assumed as perfect elastic-plastic materials that the strengths of materials remain constant after yielding.
(7) The strengthened coupling beams reach their ultimate limit state when the concrete strain at the extreme compression fiber has reached the ultimate value.
(8) Shear failure of strengthened coupling beams is not considered as the beam span-to-depth ratio is assumed to be higher than 2.

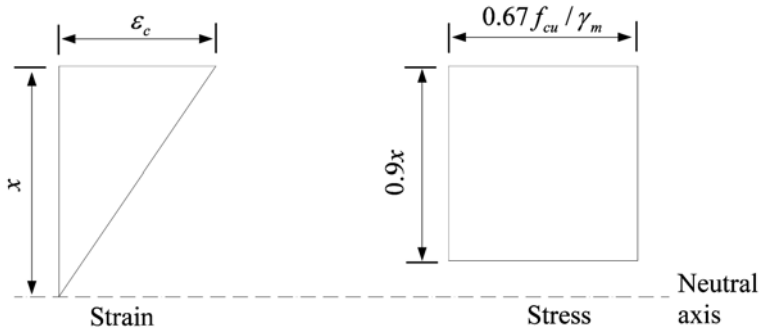

Fig. 7 Simplified stress block for concrete at the ultimate limit state

When determining the theoretical moment capacity, the simplified stress block for concrete at the ultimate limit state provided in BS8110 (1997) (as shown in Fig. 7) was adopted. A factor of 0.67 is commonly used in ultimate strength RC design to relate the less confined and less compacted concrete in a RC beam with the better confined and more complete compaction of concrete for cube compressive tests. The bi-linear stress-strain curve of steel with constant stress after yielding was used. The material partial safety factor (γ_m) of concrete and steel were taken as 1 in the analyses. The ultimate strain of compressive concrete (ε_c) is determined from the following equation (Kwan *et al*. 2001, Cheng 2001).

$$\varepsilon_c = \frac{3.46 f_{cu}^{3/4}}{E_c} \tag{37}$$

The theoretical ultimate moment capacity (M_u^*) of strengthened coupling beams is calculated under the following two situations: (1) where there is a full-interaction between the steel plate and the RC coupling beam, an upper bound estimation $M_{u,fsc}^*$ using the rigid plastic analysis method will be applied, and (2) when there is a partial-interaction between the steel plate and the RC coupling beam, the best estimate of $M_{u,psc}^*$ is produced by the mixed analysis method.

Under the assumption of full composite action between the steel plate and the RC part, the strain profiles of the concrete and the plates would be the same as shown in Fig. 5. The distance of the neutral axis from the extreme compression fiber (x) at the ultimate limit state is obtained from an equilibrium of forces, where the compression on the longitudinal reinforcement ($\overleftarrow{F}_s$), the concrete ($\overleftarrow{F}_c$), the plates ($\overleftarrow{F}_p$), the tension on the longitudinal reinforcement ($\overrightarrow{F}_s$) and the plates ($\overrightarrow{F}_p$) are as follows

$$\overleftarrow{F}_s = A_{sc} f_{ys} \tag{38}$$

$$\overleftarrow{F}_c = 0.67 f_{cu} \times 0.9 bx \tag{39}$$

$$\overleftarrow{F}_p = x.f_{yp} \times 2t \tag{40}$$

$$\overrightarrow{F}_s = A_s f_{ys} \tag{41}$$

$$\overrightarrow{F}_p = (h-x).f_{yp} \times 2t \tag{42}$$

Hence, by equilibrium of forces

$$\overleftarrow{F}_s + \overleftarrow{F}_c + \overleftarrow{F}_p = \vec{F}_s + \vec{F}_p \tag{43}$$

The depth of the neutral axis x can be determined from Eq. (43). Knowing the position of the neutral axis, the theoretical moments of the longitudinal reinforcement (M_s^*), the concrete (M_c^*) and the plates (M_p^*) about the neutral axis at ultimate limit state are added together to obtain $M_{u,fsc}^*$, where

$$M_s^* = \vec{F}_s(d-x) + \overleftarrow{F}_s(x-(h-d)) \tag{44}$$

$$M_c^* = \overleftarrow{F}_c \times 0.55x \tag{45}$$

$$M_p^* = 0.5 \times \vec{F}_p(h-x) + 0.5 \times \overleftarrow{F}_p x \tag{46}$$

Hence, by equilibrium of moments

$$M_{u,fsc}^* = M_s^* + M_c^* + M_p^* \tag{47}$$

and

$$P_{fsc} = (h-x) f_{yp} \times 2t - x f_{yp} \times 2t \tag{48}$$

When there is a partial-interaction between the steel plates and the RC coupling beam, the strain profiles of the concrete and the steel plates do not coincide. The strain and stress diagrams of the section at ultimate limit state are shown in Fig. 8. The distance of the neutral axis from the extreme compression fiber (x) at the ultimate limit state is also obtained from considering equilibrium of forces, where the compression on the longitudinal reinforcement ($\overleftarrow{F}_s$), the concrete ($\overleftarrow{F}_c$), the plates ($\overleftarrow{F}_p$), the tension on the longitudinal reinforcement ($\vec{F}_s$) and the plates ($\vec{F}_p$) are expressed as follows

$$\overleftarrow{F}_s = A_{sc} E_s \varepsilon_{sc} \tag{49}$$

$$\overleftarrow{F}_c = 0.67 f_{cu} \times 0.9bx \tag{50}$$

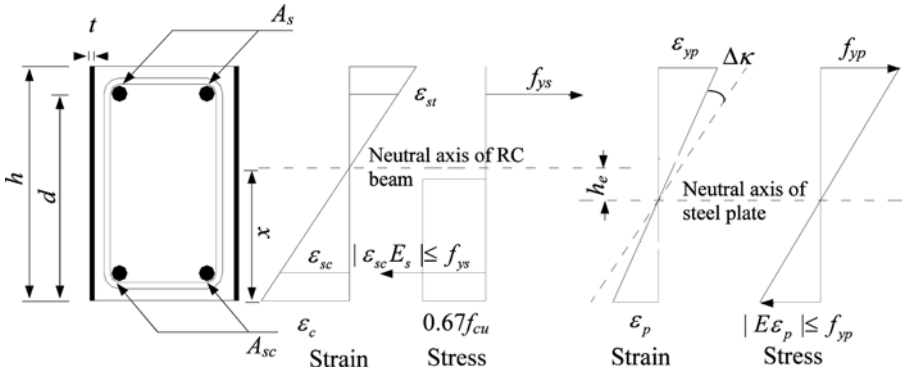

Fig. 8 Strain and stress diagrams of a section at the ultimate limit state

$$\overleftarrow{F}_p = \frac{1}{2} \times \frac{(\varepsilon_c - \Delta\kappa x)}{x}(x - h_e)^2 E_P \times 2t \tag{51}$$

$$\vec{F}_s = A_s f_{sy} \tag{52}$$

If the extreme tension fiber of the steel plate is elastic so that $\left|\frac{\varepsilon_c - x.\Delta\kappa}{x}(h - x + h_e)\right| \le \varepsilon_{yp}$, then

$$\vec{F}_p = \frac{1}{2} \times \frac{\varepsilon_c - x.\Delta\kappa}{x}(h - x + h_e)^2 E_P \times 2t \tag{53a}$$

On the other hand, if the extreme tension fiber of the steel plate is plastic so that $\left|\frac{\varepsilon_c - x.\Delta\kappa}{x}(h - x + h_e)\right| \ge \varepsilon_{yp}$, then

$$\vec{F}_p = (h - x + h_e) f_{yp} \times 2t - \frac{1}{2} \times \frac{\varepsilon_{yp}}{\varepsilon_c - x.\Delta\kappa} x.f_{yp} \times 2t \tag{53b}$$

Based on the fact that there would be no unbalanced axial force on the section, i.e.

$$\overleftarrow{F}_s + \overleftarrow{F}_c + \overleftarrow{F}_p = \vec{F}_s + \vec{F}_p \tag{54}$$

The maximum values of h_e and $\Delta\kappa$ in Eq. (54) can be related to the maximum vertical slip and longitudinal slips at the beam-wall joints by Eqs. (36) and (30) respectively. The depth of the neutral axis x can then be obtained from Eq. (54). Knowing the value of the neutral axis, the theoretical moments of the longitudinal reinforcement (M_s^*), the concrete (M_c^*) and the plates (M_p^*) about the neutral axis at the ultimate limit state can be obtained as

$$M_s^* = \vec{F}_s(d - x) + \overleftarrow{F}_s(x - (h - d)) \tag{55}$$

$$M_c^* = \overleftarrow{F}_c \times 0.55x \tag{56}$$

if, $\left|\frac{\varepsilon_c - x.\Delta\kappa}{x}(h - x + h_e)\right| \le \varepsilon_{yp}$, then

$$M_p^* = \frac{2}{3} \times \vec{F}_p(h - x + h_e) + \frac{2}{3} \times \overleftarrow{F}_p(x - h_e) \tag{57a}$$

if $\left|\frac{\varepsilon_c - x.\Delta\kappa}{x}(h - x + h_e)\right| \ge \varepsilon_{yp}$, then

$$M_p^* = 0.5 \times (h - x + h_e)^2 f_{yP} \times 2t - 0.5 \times \left(\frac{\varepsilon_{yp} x}{\varepsilon_c - \Delta\kappa x}\right)^2 f_{yP} \times 2t \times \frac{2}{3} + \frac{2}{3} \times \overleftarrow{F}_p(x - h_e) \tag{57b}$$

$$P_{psc} = \vec{F}_P - \overleftarrow{F}_P \tag{58}$$

$$M_{RC}^* = M_c^* + M_s^* \tag{59}$$

M_p^* is a function of variables h_e and $\Delta\kappa$. The theoretical ultimate moment capacity of the strengthened coupling beam can be obtained as

$$M_{u,psc}^* = M_s^* + M_c^* + M_p^* \tag{60}$$

Assuming the vertical slip of the bolt connection group at the end of the strengthened coupling

beam is S_v, the longitudinal slip is S_L at the ultimate limit state and the rotation effect of bolt connection group is θ, then from Eq. (54), the equilibrium condition; Eq. (30), the vertical slip condition; and Eq. (36), the longitudinal slip condition, the depth of concrete compression x, the maximum difference of curvatures $\Delta\kappa$ and the maximum difference of neutral axes h_e can be solved for. It is noted that non-linear slip responses of bolt groups (i.e., S_v, S_L and θ) might be obtained from the non-linear analyses (Su and Siu 2007, 2009), of which the discussion of the formulations is outside the scope of this paper. Finally, the theoretical predicted value of $M^*_{u,psc}$ can be obtained and the value of P_{psc} can be calculated according to Eq. (58).

Moreover, the total shear connection strength demand of the anchor-bolt group at the ends of the strengthened coupling beam can be estimated. The upper bound value is

$$V_{fsc} = P_{fsc} + 2\frac{M^*_{P,fsc}}{d_b} + 2\frac{M^*_{P,fsc}}{L} \tag{61}$$

Similarly, the partial shear connection strength is

$$V_{psc} = P_{psc} + 2\frac{M^*_{P,psc}}{d_b} + 2\frac{M^*_{P,psc}}{L} \tag{62}$$

As presented in the experimental study (Zhu *et al.* 2007) and in this theoretical study, a proper anchor bolt design is of vital importance to the performance of a strengthened coupling beam with steel plates. For a proper distribution of an in-plane moment and shear loads to the group of anchors, all anchors should be mobilized to take up shear loads, and undesirable slips of bolts in the clearance holes should be avoided. To achieve that, the bolts can be welded to steel plates or the clearance holes can be filled with injected adhesive mortar by using dynamic set washers. For safety considerations, the upper bound value (V_{fsc}) of the strength of bolt group from Eq. (61) can be taken as the characteristic design value of shear connection strength in bolted side plate strengthened coupling beams at the ultimate limit state. Since the anchor bolt group is often located on a wall panel, which is far from the edge of the wall and constrained by steel bars, a check of the characteristic concrete edge failure resistance (concrete breakout) need not to be considered.

The number of anchor bolts (n_V) to resist the shear force V_{fsc} under steel failure is

$$n_V V_{R,s} \geq V_{fsc} \quad (n_V \geq 4) \tag{63}$$

The shear capacity $V_{R,s}$ of a single anchor according to ACI 349 (2001) can be obtained as

$$V_{R,s} = 0.6 A_{s,a} f_{u,s} \tag{64}$$

where $A_{s,a}$ is the area of cross section of the anchor and $f_{u,s}$ is the characteristic steel ultimate tensile strength.

The resistance to concrete pryout failure ($N_{R,cp}$) in the anchor group must be verified and must satisfy the following equation.

$$N_{R,cp} \geq V_{fsc} \tag{65}$$

According to ACI 349 (2001), the corresponding characteristic resistance $V_{R,cp}$ may be calculated as

$$V_{R,cp} = 20.16\sqrt{f_{cu}}.h_{ef}^{1.5}.\frac{A_{c,N}}{A^0_{c,N}} \tag{66}$$

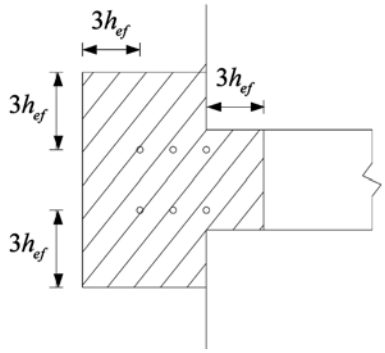

Fig. 9 Example of actual area of $A_{c,N}$ for Unit CB4

Here f_{cu} is the concrete cubic compression strength, h_{ef} is the effective anchorage depth (half thickness of shear wall for a through anchor), $A^0_{c,N}$ is the area of concrete of an individual anchor with large spacing and edge distance at the concrete surface, $A_{c,N}$ is the actual area of concrete cone of the anchorage at the concrete surface.

$$A^0_{c,N} = 9h^2_{ef} \tag{67}$$

$A_{c,N}$ is limited by overlapping concrete cones of adjoining anchors as well as by the edges of the concrete member. Examples for calculating of $A_{c,N}$ are illustrated in Fig. 9.

4.2 Application of the developed models

An experimental study of strengthening coupling beams with bolted side steel plates has been presented in the companion paper (Zhu *et al.* 2007). Four specimens (Units CB2 to CB5) of strengthened coupling beams with a same span depth ratio ($l/h = 2.5$), identical dimensions and reinforcement details, but with different strengthening arrangement were tested. The experimental study showed that the present external attachment of steel plates can effectively improve the strength and deformability of coupling beams. Unit CB2 had bolt connections along the span of the beam where the theory has not been taken into account and Unit CB3 had premature damage of bolt connections in the bolt group during the test. Therefore, for illustration and validation purposes, the experimental results of Unit CB4 and Unit CB5 were selected for comparison with results from the theoretical study.

4.2.1 Rigid plastic model

As described in Section 3, the rigid plastic model is used for the determination of the upper bound strength of strengthened coupling beams with bolted side steel plates. The upper bound strength of Units CB4 and CB5 was calculated according to equations (43, 47 and 48) and the results have been presented in Table 1. It can be seen from the table that the upper bound values of the strengthened coupling beams are much higher (by up to 41%) than those from the experimental test as the effect of slip of bolt groups has not been considered in the rigid plastic model. Despite the inaccuracies of the prediction, the upper bound value obtained from rigid plastic model may be conservatively and conveniently used to estimate the characteristic design forces for the design of shear connections.

Table 1 Key calculation details for Units CB4 and CB5 by rigid plastic model

	x (mm)	$M^*_{u,fsc}$ (kN.m)	P_{fsc} (kN)	$V^*_{u,fsc}$ (kN)	V_{test} (kN)	$V^*_{u,fsc}/V_{test}$
Unit CB4	57.6	164.1	171.9	437.7	354.0	1.24
Unit CB5	87.4	221.6	243.3	590.9	418.0	1.41

Table 2 Key calculation details for Units CB4 and CB5 by mixed analysis model

	S_L (mm)	S_V (mm)	θ (Rad)	x (mm)	$M^*_{u,psc}$ (kN.m)	P_{psc} (kN)	$V^*_{u,psc}$ (kN)	V_{test} (kN)	$V^*_{u,psc}/V_{test}$
Unit CB4	0.25	0.47	0.005	57.1	135.6	171.9	372.4	354.0	1.05
Unit CB5	0.43	0.63	0.006	81.3	162.8	243.3	448.9	418.0	1.07

4.2.2 Mixed analysis model

The mixed analysis model, in which the slip and rotation effects of the bolt connection group are considered, can be used to analyze the actual strength of strengthened coupling beams. In the strength analysis, the theory of the nonlinear response of bolt groups (Su and Siu 2007 or Siu and Su 2009) might be used for determining the slips and rotation angle of bolt connection groups. In this method, the bolts were assumed to behave in an elasto-plastic manner and the bolt group was moved as a rigid body. An iterative procedure, which was developed by Su and Siu (2007), was used to calculate the instantaneous centre of rotation of the bolt group and the full range non-linear response of bolt groups subjected to in-plane loads was simulated. Based on Equations (30, 36, 54, 58, 60), the load-carrying capacity of Units CB4 and CB5 was determined and is presented in Table 2. It is found that the steel plates in Unit CB4 are more efficient than those in Unit CB5 due to less slip and less rotation of the bolt connections. Comparing Tables 1 and 2, the strength predicted by the mixed analysis model, which accounts for the longitudinal and vertical slips, produces more accurate results than the rigid plastic model, with less than 7% errors.

5. Conclusions

The theoretical models based on the rigid plastic and mixed analysis for medium-length side bolted steel plate strengthened coupling beams have been developed. The equations derived from these models, in which the influence of cyclic loads is not accounted for, can be used for the determination of the ultimate strength of steel plate strengthened RC coupling beams with bolt connections. The mixed analysis model considered the effect of longitudinal and vertical slips and the rotation of bolt connection groups, making it superior to the rigid plastic model. The strength of the strengthened coupling beams predicted by this model is in good agreement with that of the experimental results. In practice, this theoretical model can assist the designers to calculate the required thickness of the steel plate and the number of anchor bolts to achieve the required strength with a given type of anchor bolt.

Acknowledgements

The first author would like to thank for the partial support of this project from The Bureau of Science and Technology of Guangzhou (Project No. 9451009101003185). The second author would like to thank for the partial support of this project from the Research Grants Council of Hong Kong (Project No. HKU7168/06).

References

ACI Committee 349 (2001), "Code requirements for nuclear safety related concrete structures (ACI-349-01) and Commentary (ACI 349R-01)", American Concrete Institute, Michigan.

BSI (1997), "BS8110 Part 1: Code of practice for design and construction, structural use of concrete", British Standards Institution 1985, London.

Cheng, L.S.B. (2001), "Stress-strain curve of concrete under compression", Research Project Report (2000-2001), Department of Civil Engineering, The University of Hong Kong.

Johnson, R.P. (1994), *Composite Structures in Steel and Concrete*, Blackwell Scientific, Oxford.

Kwan, A.K.H., Lee, P.K.K. and Zheng, W. (2001), "Elastic modulus of normal and high strength concrete in Hong Kong", *Transact. Hong Kong Institut. Eng.,* **8**(2), 10-15.

Newmark, N.M., Siess, C.P. and Viest, I.M. (1951), "Tests and analysis of composite beams with incomplete interaction", *Proc. Soc. Experim. Stress A.,* **9**(1), 75-92.

Oehlers, D.J. (1992), "Reinforced concrete beams with plates glued to their soffits", *J. Struct. Eng-ASCE*, **118**(8), 2023-2038.

Oehlers, D.J. and Bradford, M.A. (1995), *Composite Steel and Concrete Structural Members: Fundamental Behavior*, Pergamon Press, Oxford.

Oehlers, D.J. and Bradford, M.A. (1999), *Elementary Behavior of Composite Steel and Concrete Structural Members*, Butterworth Heinemann, Oxford.

Oehlers, D.J. and Sved, G. (1995), "Flexural strength of composite beams with limited slip capacity shear connectors", *J. Struct. Eng-ASCE*, **121**(6), 932-938.

Oehlers, D.J., Nguyen, N.T. and Ahmed, M. (1997), "Transverse and longitudinal partial interaction in composite bolted side-plated reinforced-concrete beams", *Struct. Eng. Mech.*, **5**(5), 553-563.

Siu, W.H. and Su, R.K.L. (2009), "Load-deformation prediction for eccentrically loaded bolt groups by a kinematic hardening approach", *J. Constr. Steel Res.,* **65**(2), 436-442.

Su, R.K.L. and Siu, W.H. (2007), "Nonlinear response of bolt groups under in-plane loading", *Eng. Struct.*, **29**(4), 626-634.

Zhu, Y., Su, R.K.L. and Zhou, F.L. (2007), "Seismic behavior of strengthened reinforced concrete coupling beams by bolted steel plates, Part 1: Experimental study", *Struct. Eng. Mech.*, **27**(2), 149-172.